Image Cover Sheet

CLASSIFICATION	SYSTEM NUMBER
UNCLASSIFIED	510327

TITLE

THE MEASUREMENT OF ELASTIC STRAIN FIELDS AND LINE-BORADENING NEAR CRACKS IN LOADED BARS OF HY-80 STEEL

System Number:

Patron Number:

Requester:

Notes: Paper #22 contained in Parent Sysnum #510305

DSIS Use only:

Deliver to: DK

THE MEASUREMENT OF ELASTIC STRAIN FIELDS AND LINE-BROADENING NEAR CRACKS IN LOADED BARS OF HY-80 STEEL

by

T.M. Holden, J.H. Root and J.F. Mecke

AECL Research, Chalk River, Ontario Canada K0J 1J0

and

J. Porter, Defence Research Establishment Atlantic, Halifax, N.S. B3K 2X0

ABSTRACT

The elastic strain fields in the neighbourhood of 6 mm and 20 mm deep cracks in bars loaded in three-point bending were measured by neutron diffraction. Calculations of the elastic strain field under the known loads included a stress-concentration contribution approximated by linear elastic fracture mechanics (LEFM). Close to the crack tip, the calculated load-induced strains with the LEFM contribution are in reasonable agreement with the measurements although the agreement is not good far from the crack. The diffraction linewidths can be related to the plastic deformation within the region of measurement. A 20% increase in linewidth occurred ahead of and behind the crack tip, and near the uncracked surface adjacent to the central support for the three-point bending. The radius of the enhanced linewidth region was about 5 mm near the crack tip.

1. INTRODUCTION

Recent engineering studies at the Defence Research Establishment Atlantic[1] (DREA) have established that plastic zone development around cracks takes on two distinct patterns depending on whether the crack is deep or whether it is shallow. For deep cracks the plastic zone first develops under load on or near the surface ahead of the crack, whereas for shallow cracks the pattern develops on the surface behind the crack. When the plastic pattern breaks to the top surface, the surface yields and two plastic hinges develop, one on either side of the crack. The surface plastic strains have been measured experimentally by the distortion of photo-etch patterns.

The purpose of the present experiments was twofold. First to measure the elastic strain fields near cracks under load by neutron diffraction and secondly to test whether it is feasible to identify the plastic zones near cracks at depth in the material by line-broadening of the diffraction lines. Two samples were studied with cracks penetrating 6 and 20 mm through the 40 mm thickness of the bar in order to characterize the differences between shallow and deep crack behaviour.

In order to have conventional measurement of the surface stress and in order to assess the applied loads, the samples were instrumented with strain gauges and a calibration experiment was carried out with known loads on an MTS-810 testing machine. Firstly the plastic load limit[2] was calculated for each sample, and then each sample was loaded in 3-point bending to 50% of this limit in the MTS-810 testing machine while monitoring the strain gauges.

Subsequently the sample were placed in a clamp-type three point bending rig supplied by DREA and mounted on the L3 spectrometer at the NRU reactor. Measurements were made at zero load, about half the calibrated load, and at the full calibrated load for each sample. Finally the shallow-crack sample was strained to 80% of the plastic load limit. Measurements of the axial strain response to the applied axial load in 3-point bending were made at the mid-width position as a function of through-thickness location and axial displacement from the crack on a 4mm grid. The diffraction line-broadening was obtained on the same grid.

The present paper summarizes and discusses the experimental findings and is organized as follows: the detailed description of the samples is given in Section 2, the neutron diffraction experiments are described in Section 3, the appropriate theory is reviewed in Section 4 and the results are presented, analyzed and discussed in Section 5.

2. SAMPLES

The samples of high strength low alloy steel were bars 254 mm long, 25.4 mm wide and 40.0 mm thick. The shallow crack, as seen at the surface, penetrated 6mm into the thickness, while the deep crack penetrated 20mm into the thickness. Each sample was instrumented with strain gauges as shown in the sketch of the 6 mm crack sample in Fig 1 which gives the position of each gauge.

The plastic load limit[2] P_L, the load at which the plastic zones from top and bottom surfaces first join, is given by

$$P_L = \frac{4}{3} b W_{RL}^2 \frac{Y}{S} \quad (1)$$

where b is the width of the test piece 24mm, W_{RL} is the thickness of the remaining ligament (34 and 20mm for the shallow and deep crack respectively), Y is the yield strength (80ksi,551.6MPa) and S is the span between supports in a 3-point bend test, 207mm. The plastic load limits were 36.1 kN for the deep crack and 104.3 kN for the shallow crack.

The samples were loaded to 50% of P_L in an MTS-810 testing machine in 5 kN steps for the 6mm crack and 2kN steps for the 20mm crack measuring the strains with strain gauges at each step. The samples were unloaded in the same steps and the strains remeasured to provide a calibration of the strain gauges. The load was ascertained in the neutron experiments by reading the calibrated strain gauges.

3. NEUTRON SCATTERING EXPERIMENTS

The neutron scattering experiments were carried out in the clamp-type 3-point bending rig which is shown mounted on the L3 spectrometer at the NRU reactor in Figure 2. The component of strain measured is along the length of the bar which corresponds to the elongation of the "fibres" of metal caused by the 3-point bending.

The wavelength of neutrons, 2.4824±0.0001Å, produced by reflection from the (113) planes of a Ge single crystal monochromator, was calibrated with Si powder from the National Institute for Standards and Technology. The (110) planes of the body-centred cubic structure of the steel give a diffraction peak near $2\theta \approx 75°$. The instrumental angular width for this experiment has to be minimized in order to see line-broadening effectively and this setup represents a design compromise in the experiment between the angular width of the diffraction peak and the spatial resolution of the experiment. The minimum width observed was 0.44±0.01 deg. The region of intersection of the incident and scattered beams, the gauge volume, over which the strain and widths are averaged in the measurement, was defined by slits of width 2mm and height 2mm in absorbing cadmium placed in the incident and scattered beams.

The lattice spacing for the (110) planes, d_{110}, is related to the diffraction angle $2\theta_{110}$ and the known neutron wavelength, λ, by Bragg's law

$$\lambda = 2d_{110}\sin\theta_{110}. \qquad (2)$$

The strain is calculated with respect to lattice spacings far from the crack under zero load, d^{o}_{110}, as follows:

$$\epsilon_{110} = (d_{110} - d^{o}_{110}) \,/\, d^{o}_{110}. \qquad (3)$$

The values of the reference spacings for the 6mm crack and 20mm crack samples, are 2.0332(1) and 2.0331(1) Å respectively. The measured linewidths, Δ_m in degrees, of the diffraction peaks (FWHM) are determined from the fitted widths

of the Gaussian lineshape. The linewidths far from the crack define the values of reference linewidths, Δ_r, which are principally due to the experimental resolution of the instrument with an intrinsic component from the manufacture of the crack. To determine an intrinsic width the reference linewidth is subtracted from the measured linewidth in quadrature as follows:

$$\Delta^2 = \Delta_m^2 - \Delta_r^2 \tag{4}$$

The root mean square strain is obtained by differentiating Bragg's law and is given in terms of the intrinsic FWHM, Δ, by

$$\left[\frac{\Delta d}{d}\right]_{rms} = \cot\theta \, \frac{.\pi\Delta}{720} \tag{5}$$

where the numerical factors convert from degrees at half maximum, to the standard deviation.

The measurements were made at zero load (with the 3-point bending rig just holding the sample) and two higher loads approximately 25 and 50% of P_L for each sample as determined by the gauge readings. In a final experiment the 6mm crack sample was taken to 80% of the plastic load limit, approximately 30% beyond the calibration in an attempt to generate more dramatic effects.

3.1 Linear Elastic Fracture Mechanics

The elastic stress field ahead of a sharp crack calculated within the theory of Linear Elastic Fracture mechanics is given by[3]

$$\sigma_x = \frac{K_I}{\sqrt{2\pi r}} \cos\frac{\theta}{2}\left\{1 - \sin\frac{\theta}{2}\cos\frac{3\theta}{2}\right\} \quad (6)$$

$$\sigma_y = \frac{K_I}{\sqrt{2\pi r}} \cos\frac{\theta}{2}\left\{1 + \sin\frac{\theta}{2}\cos\frac{3\theta}{2}\right\} \quad (7)$$

The coordinate axes are given in Figure 1, with the x-axis along the direction of the crack and the y-axis perpendicular to the crack. The distance from the tip is designated r and θ is the angle the position makes with the x-axis. In the approximation of plane stress, which would hold for thin sections or near the surface of the bars, σ_z is set equal to zero. In the interior of the bar, plane strain conditions would approximately hold, $\epsilon_z = 0$. In this case

$$\sigma_z = \nu(\sigma_x + \sigma_y) \quad (8)$$

where ν is Poisson's Ratio.

The constant K_I is the stress intensity factor which depends on the geometry of the crack and the nature of the load, e.g. bending or uniaxial stress. For the case of 3-point bending, we may use the equation for K_I given by Broek[4]

$$K_I = \frac{PS}{bW^{3/2}}\left\{2.9\left(\frac{a}{W}\right)^{1/2} - 4.6\left(\frac{a}{W}\right)^{3/2} + 21.8\left(\frac{a}{W}\right)^{5/2} - 37.6\left(\frac{a}{W}\right)^{7/2} + 38.7\left(\frac{a}{W}\right)^{9/2}\right\} \quad (9)$$

where P is the load (kN), S is the span between the supports, 0.207m, W is the beam thickness, a is the crack length and b is the width of the bar. K_I has the value 51.3MPa.$\sqrt{m}$ for a 50.2kN load on the 6mm crack sample and 48.5 MPa.$\sqrt{m}$

for a 17.8kN load on the 20mm crack sample. K_I scales with load for the same geometry.

The expression for the strain ϵ_y in the axial direction which is measured in the experiment is

$$\epsilon_y = \frac{1}{E} (-\nu\sigma_x + \sigma_y - \nu\sigma_z) \tag{10}$$

For comparison with the strain gauges the bulk Young's modulus E and Poisson's Ratio ν are used. For comparison with the neutron results the diffraction elastic constants are used and both are given in Table 1.

To the strains generated by the stress enhancement under load at the crack tip must be added the applied strain ϵ_{app}, generated by the bending moment and this is given by

$$\epsilon_y^{app}(X,Y) = \frac{1}{E} \frac{3P}{bW^3} (S/2 - Y) (2X - W) \tag{11}$$

where Y is the axial offset from the crack position and X is the distance through the wall from the uncracked face.

Because of the divergence of the stress field near the crack tip, the value of the stress may exceed the yield point, σ_{ys}, for the material. The radius of the plastic zone, ahead of the crack may be deduced from Equation 7, setting θ=0. The size of the plastic zone is about $2r_y$. For the approximation of plane stress, i.e. near the surface

$$r_y = \frac{1}{2\pi} \left[\frac{K_I}{\sigma_{ys}}\right]^2 \tag{12}$$

and in the approximation of plane strain i.e. at depth, it is a factor of 3 smaller[3]. For HY80 the yield stress is 80ksi (551.2 MPa). For the highest load applied to the 6mm crack, P = 98.5 kN, $r_y^{surface}$ = 3.8mm and $r_y^{internal}$ = 1.3mm. For the highest load applied to the 20mm crack, P = 17.8kN, $r_y^{surface}$ = 1.2mm and $r_y^{internal}$ = 0.4mm.

To find the macroscopic surface strains under load in a flawed bar, the bar is instrumented at zero load with strain gauges. The change in gauge reading is measured as a function of applied load. This effectively takes as zero reference state the residual strain state of the bar generated by producing the crack. In the case of measurements with neutrons, the residual stress/strain in the bar caused by generating the crack is measured with respect to a reference lattice spacing far from the crack. In order to find the strain generated by loading the bar the reference state is the residual strain state of the bar.

4. RESULTS AND DISCUSSIONS

4.1 Strain Gauge Results

For strain gauges well removed from the crack, for example gauges 10-13 which are 38.1mm from the crack, the effect of the crack is expected to be small, and the strain may be calculated from the applied load. For a load of 47 kN the strain at positions 10-13 calculated with the bulk elastic constants is 10.7×10^{-4}. This compares well with the average gauge readings of

$+11.4\pm0.4\times10^{-4}$ and $-11.3\pm0.3\times10^{-4}$. Likewise for the 20mm crack sample at the maximum load of 17kN, the calculated surface strain is 3.9×10^{-4}, and the average measured surface strains from gauges 10-13 are found to be 4.0 ± 0.1 and $-4.1\pm0.3\times10^{-4}$. This good agreement between the axial strain calculated and measured far from the crack in the calibration gives confidence in calculating the applied moments in the diffraction experiments. Closer to the defect, the effect of the crack is observed. For example at position #8, 10.2mm from the crack on the tensile face, the calculated strain for the 6mm sample at a load of 47kN is $+15.2\times10^{-4}$ whereas the measured strain is 7.1×10^{-4}. The effect of the crack is still important at position #9, 20.3mm from the crack, where the calculated strain is 13.5×10^{-4} and the measured strain is 12.1×10^{-4}.

Turning now to the strain gauge measurements made during the neutron scattering experiments, we use the strains measured on the gauges to calculate the surface stresses knowing the bulk Young's modulus. From the actual beam dimensions and the actual gauge locations, with no calibration factor, we may calculate the loads, P, from Equation 11. From the measured strains in the 3-point bending rig at positions 10-13, far from the crack, we have deduced that the applied loads were 23.5,50.2 and 83.4 kN for the 6mm crack sample and 8.6 and 17.8kN for the 20mm crack sample with an accuracy of ±3%. This accuracy was determined from the spread in strain gauge readings.

4.2 Strains Measured by Neutron Diffraction

The measured strains for the 6mm crack sample at loads of 0, 23.5, 50.2 and 83.4kN are shown as contour maps of strain as a function of position in Figure 3 for the 6mm crack sample and Figure 4 for the 20mm crack sample. Some measurements were made on both sides of the crack to check for symmetry and there was good agreement in these cases. However the data were mainly obtained on one side of the crack. The contour maps of strain are reflected about the line of the crack for ease of visualization.

Several features are noticeable immediately in Figure 3. Behind the crack the axial strain is compressive and independent of the load. A maximum of 4×10^{-4} in residual strain is noted 4mm ahead of the crack in the unloaded specimen. Under load the tensile strain ahead of the crack increases strongly, and at the same time a compressive strain develops on the opposite face. The maximum compressive strain was not found under the central support roller, but displaced 5-10mm to the side. The support roller is thus, in some sense, acting as a constraint in the development of the compressive strain. We believe that this feature would be absent in 4-point bending. The axial gradient of the strain is weak except close to the crack and near the support point.

The same general features are evident in the results for the 20mm crack; in Figure 4 the maximum in strain lies well ahead of the crack tip which comes at X=20mm. A compressive strain is observed behind the crack tip which is nearly

independent of load. The behaviour near the support point at the compressive face is complex.

For detailed comparison with linear elastic fracture mechanics and with the strain gauge results we have subtracted off the residual elastic strain (Figure 5 and Figure 6) from the total strain under load. The results for the 6mm crack sample under loads of 50.2 and 83.4kN are shown in Figure 7 and the 20mm crack sample under a load of 17.8kN in Figure 8. The solid lines in each case are the calculated strain from the known loads applied in bending using the diffraction elastic constants for the (110) reflection. The short-dashed lines are the sum of the applied strain and the strains from the stress-enhancement, Equations 6 & 7, in the neighbourhood of the crack. At positions well removed from the crack i.e. 30, 50 mm, the applied strain gives an excellent description of the neutron results, and the dashed curve is in disagreement with the measured strains. We recall that the difference between the dashed and solid curves is the elastic stress field calculated within linear elastic fracture mechanics, Equations 6 and 7. This term is felt a long way from the crack tip because of the slow fall-off of the $1/\sqrt{r}$ term in Equations 6 and 7. This, therefore, appears to be a defect in the theory. It is interesting to note that the slope of the line at 50mm is less than at 30mm, since the moment is smaller in 3-point bending further away from the centre of the span.

Closer to the crack, at 8mm and 16mm, the calculated applied strain is less than the measured compressive strain near the compressive face, but is greater than the strain ahead of the crack. The applied strain line overestimates the

strain behind the crack (shown dashed here) since the crack cannot support an axial stress. The deviations from the applied load behaviour are a maximum near the crack. The most dramatic effects are seen in the case of the largest applied load. The prediction of linear elastic fracture mechanics, shown dotted, overestimates the magnitude of the elastic strain. The strain gauge results of the total surface strain, elastic plus plastic, are included in Figures 7 & 8 and it is seen that there is good qualitative agreement between them and the elastic diffraction strains where they may be directly compared even though they are in different physical locations and even though strain gauges measure the total elastic plus plastic strain.

In retrospect it would have been a better procedure to measure the residual strain in the samples before loading the samples in the MTS-810 testing machine. This would have settled without any doubt that the residual strains originate in the fabrication of the fatigue crack. At present we have not proved that this is the cause of the residual strains although this remains likely to be correct.

4.3 Linewidths of the Diffraction Peaks

The intrinsic linewidths of diffraction peaks may have several causes, such as high dislocation density indicating plastic deformation or cold work, or a large variation of elastic strain within the set of correctly oriented grains fulfilling the diffraction condition. In a trivial way, a strong strain gradient within the gauge volume can also generate apparent widths although the gradients obtained in the present experiments are not large enough to give

broadening. The diffraction linewidths have a magnitude between 0.4 and 0.5 deg. with a typical uncertainty of ±3%. The largest part of the linewidth originates in the instrumental resolution, and the intrinsic contributions add in quadrature. This uncertainty limits the information available from the linewidths. The results for the 6mm crack are plotted as a function of both position and load in Figure 9. The results far (20-50mm) from the crack show a significant through-thickness variation which is load independent and which presumably originates in the manufacture of the bar. The minimum linewidth is 0.445° and the scatter is statistically consistent with the estimated uncertainties. The curve drawn through the data for 20-50mm is reproduced for all the other distances as a base-line against which to measure crack or load induced effects. There are no additional contributions to the linewidth until the offset from the crack is 8mm or less. An intrinsic width is observed extending 12mm in from the compressive face at a load of 83.4kN. At a displacement of 4mm from the centreline an intrinsic width which appears to be load <u>independent</u> is observed at the crack tip. A load-dependent contribution is observed near the compressive face. On the centreline a 20% increase of linewidth occurs at the crack tip which is independent of load. The intrinsic linewidth corresponding to the maximum increase is 0.29±0.05°, and the rms strain is $(14.3\pm2.5)\times10^{-4}$. The width increase has disappeared 5mm from the location of the maximum. A load-dependent enhancement of the width is observed at the compressive face which extends 10mm into the material at a load of 83.4kN but only 2mm for the lower loads.

We conclude that the region of enhanced width with a radius of about 5mm is the plastic zone near the crack tip, since it is load independent.

Analogous results for the 20mm crack sample are shown in Figure 10. For this sample the through-wall variation far from the crack (20-50mm) is very slight, as indicated by the curve drawn through the points which serves as a baseline for the closer distances. In this case the region of enhancement of linewidth is restricted to the results on the centreline and it has disappeared 2mm ahead of the crack and 4mm laterally displaced. A region of enhanced width extends behind the tip of the crack to the tensile face of the bar and this effect is also visible 4mm to the side of the crack. The magnitude of the enhancement at the peak is 0.29±0.02 deg [rms strain = $(14.3\pm0.9)\times10^{-4}$] and behind the crack the intrinsic width is 0.15±0.07 deg [rms strain $(7.2\pm3.6)\times10^{-4}$]. The location of the peak in width is very close to the end of the crack and is offset from the peak in the strain field. The region of enhanced width 2mm around the crack tip is tentatively identified as the plastic zone. Measurements of the peak widths for specimens with known amounts of cold work should be made in order to correlate the effects in the cracked bars with plastic damage.

It would be valuable to compare the present strain results with finite element calculations of the elastic strain field within the 3-point bending geometry. This is because the existence of the support roller opposite the crack certainly acts in a constraining fashion with a strong perturbation of the expected stress enhancement field near the compressive face. It is possible to separate out the elastic and plastic parts of the strain field in the calculation and make the appropriate comparison. Linear elastic fracture mechanics does not seem to be capable of describing the results near the crack even though the calculated plastic zone sizes (Equation 12) are quite

localized. It will be interesting to compare the predicted plastic zone size and shape with the regions of enhanced width seen in this experiment.

It would be very useful to make measurements on a photo-etched sample under load. In this way the plastic and elastic surface properties could be established and the plastic and elastic properties at depth could be found by neutron diffraction.

5.0 ACKNOWLEDGEMENTS

We wish to acknowledge the helpful advice of B.L. Wotton in making the strain gauge calibration and L.E. McEwan in preparing jigs to mount the bending rig on the spectrometer. R.H. Hosbons provided important guidance in the application of fracture mechanics.

6.0 REFERENCES

1. "A general discussion of short crack fracture", DREA discussion document, J.R. Matthews, J.F. Porter, C.V. Hyatt and K.J. Karis Allen. Proceedings of the Conference on shallow crack fracture mechanics, toughness tests and applications. Cambridge, England, 23-24 September 1992.

2. Standard Test Method for J_{ic}, a measure of fracture toughness. ASTM Standard E813-89.

3. "Fracture and Fatigue Control in Structures". S.T. Rolfe and J.M. Barsom (Prentice-Hall Inc.: New Jersey) 1977.

4. "Elementary Engineering Fracture Mechanics" D. Broek (Martinus-Nijhoof: Dordrecht) 1986.

5. D.J. Dever, J. Appl. Phys. 43, 2393 (1972.

6. E. Kröner, Z. Physik 151, 504 (1958)

TABLE 1

CALCULATED AND EXPERIMENTAL ELASTIC CONSTANTS FOR IRON

E bulk	(calc, a)	213 GPa
ν bulk	(calc)	0.288
E bulk	(experiment, b)	211 GPa
ν bulk	(experiment)	0.293
E_{110}	(calc, a)	225 GPa
ν_{110}	(calc)	0.276

a Calculated from the elastic constants for Fe[5] by the Kröner method[6]

b Smithells' Metals Reference Book, Sixth Edition, 15-5 Edited by E.A. Brandes (Butterworth and Co.)

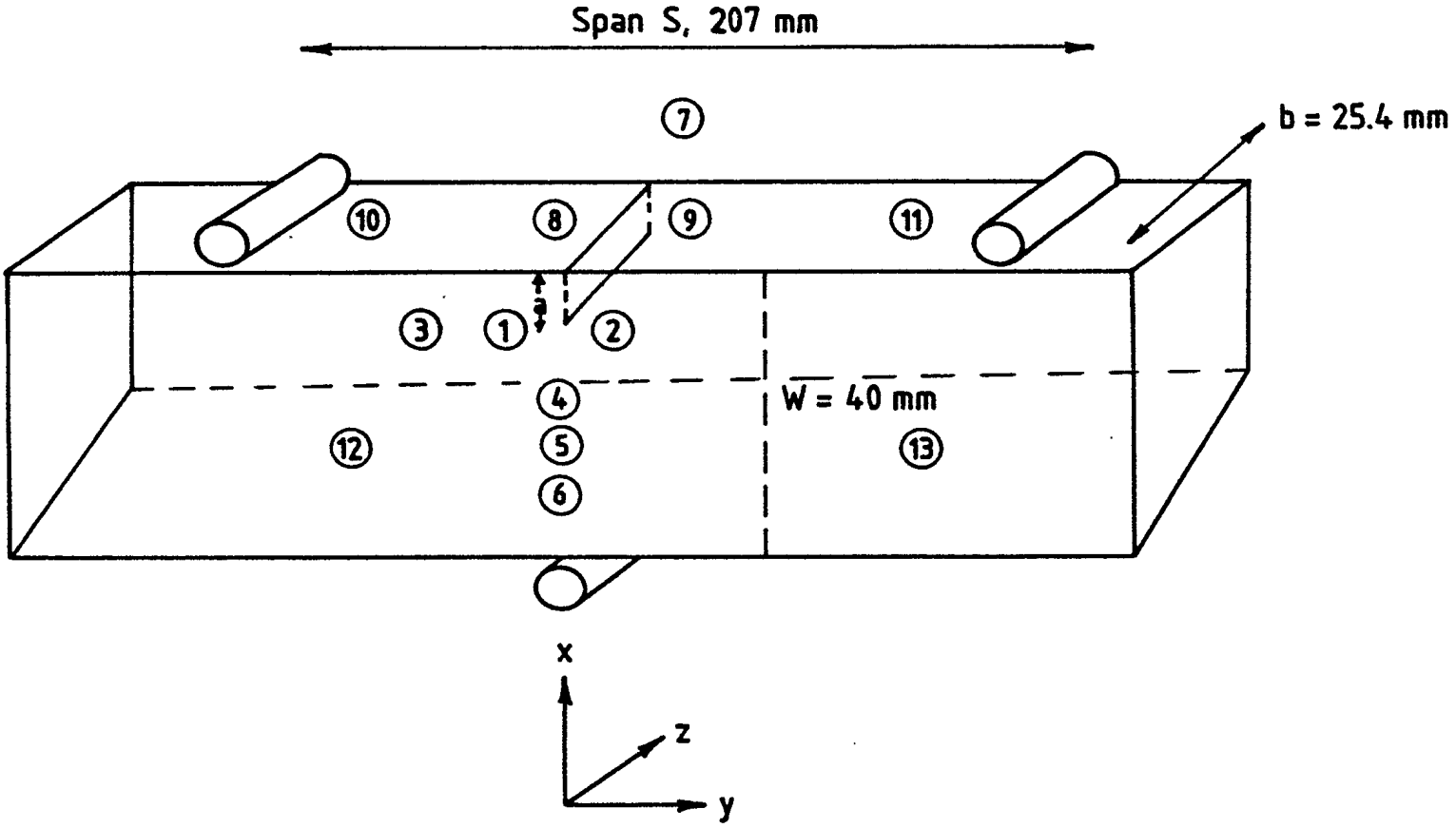

Fig. 1 Sketch of the bar, showing the location of gauges 1-13, three-point bending supports, dimensions and the coordinate scheme adopted. The strain gauges 4-6 are positioned the same distances from the crack tip for both 6mm and 20 mm crack samples. The crack is represented by a planar section penetrating into the bar and the shallow crack is shown here. The crack length, that is the penetration of the crack into the material is denoted by a.

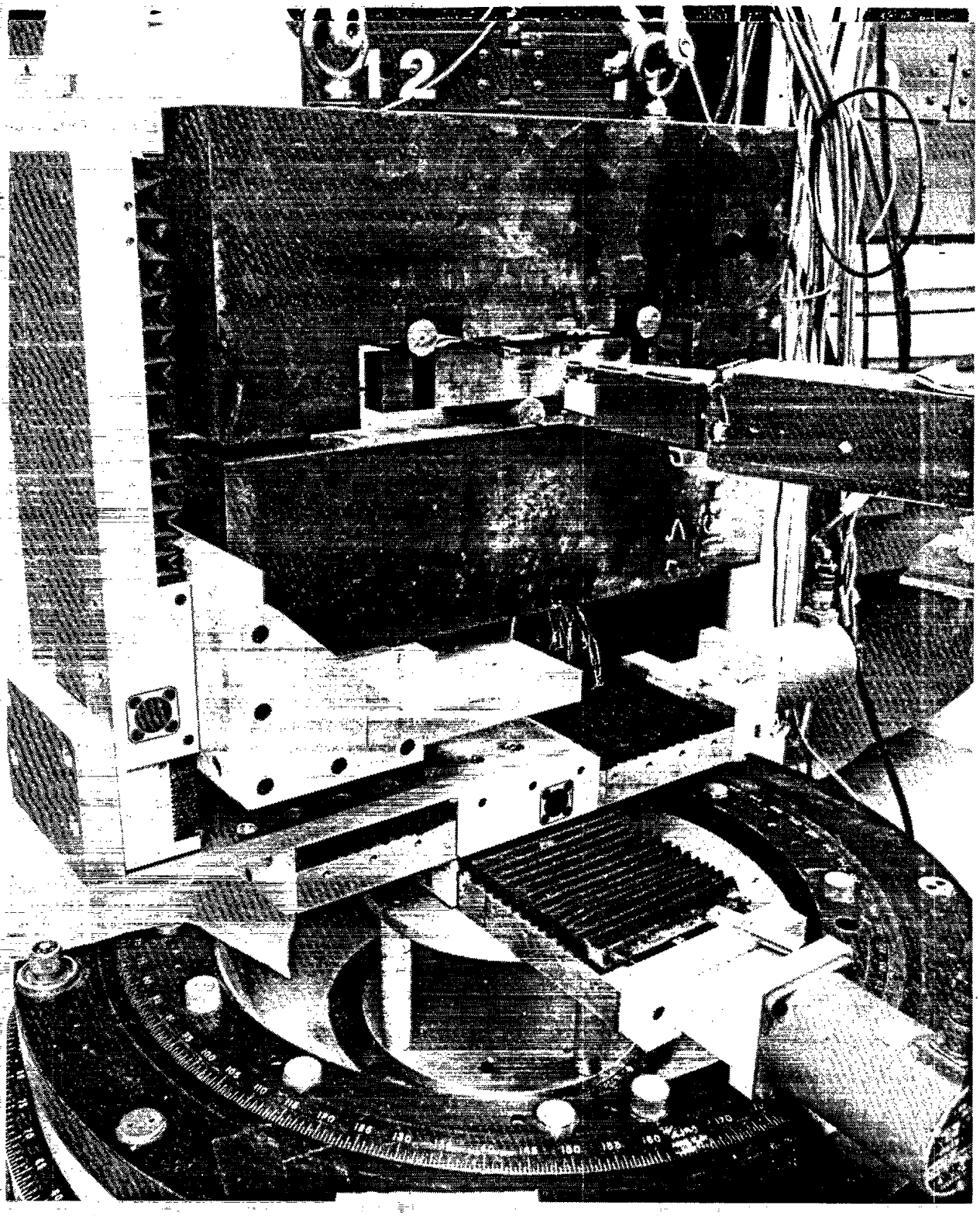

Fig. 2 Photograph of the 6 mm crack sample mounted in the 3-point bending rig on the L3 spectrometer at the NRU reactor. The X-Y-Z translator system is clearly seen supporting the rig. The snout holding the slit defining the scattered beam points at the sample from the right hand side.

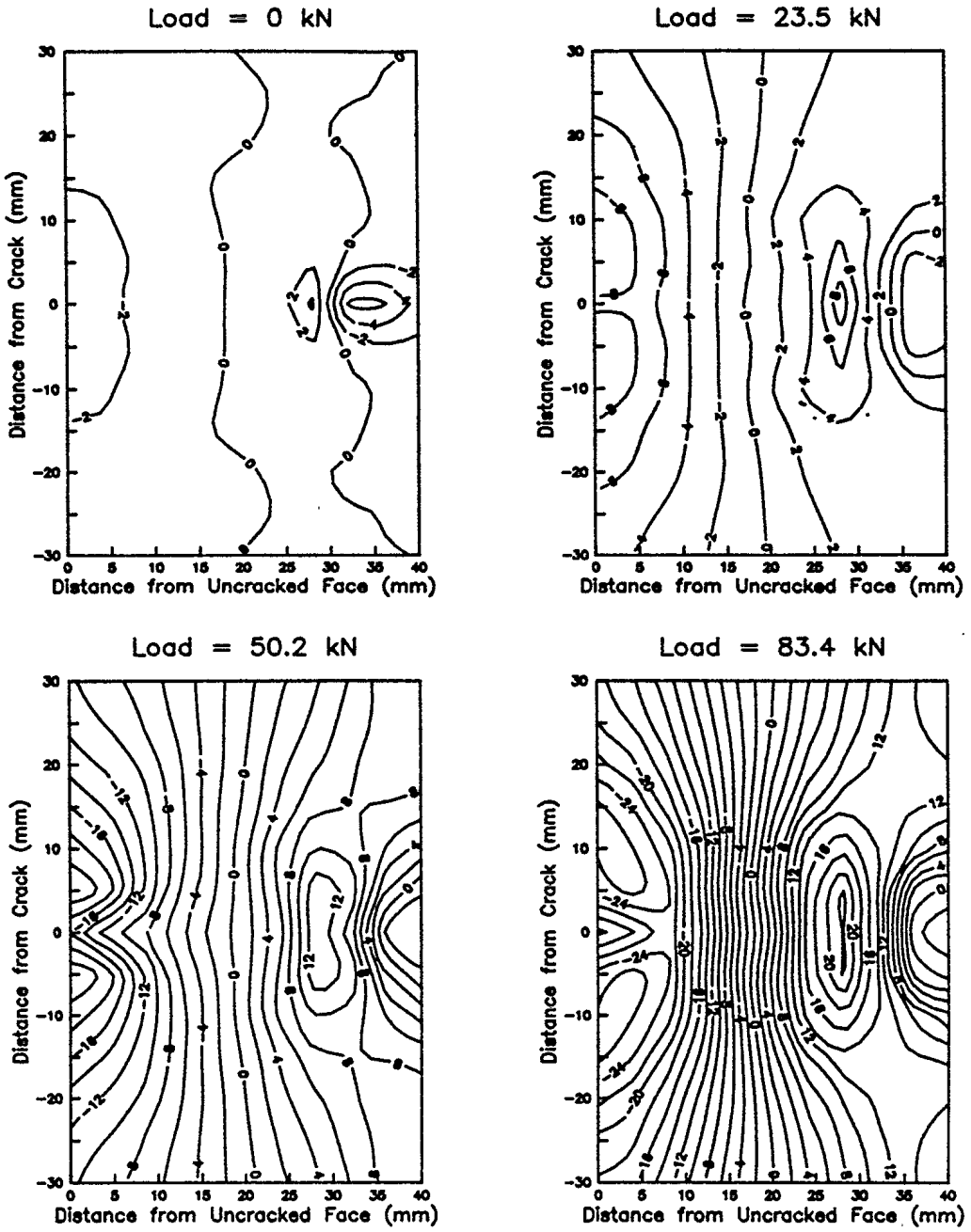

Fig. 3 Contour maps of strain as a function of distance from the uncracked face and lateral distance from the crack plane for the 6 mm crack sample at loads of 0, 23.5, 50.2 and 83.4 kN.

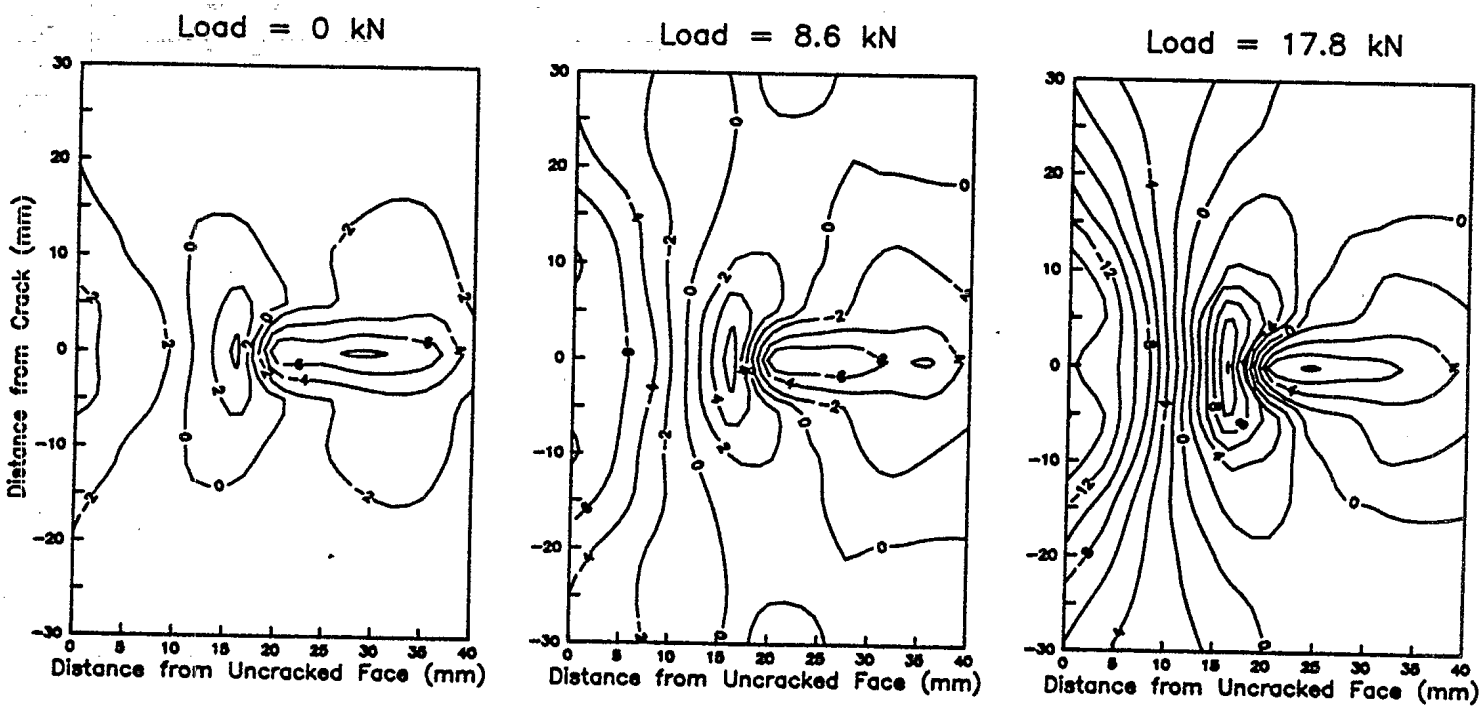

Fig. 4 Contour maps of strain as a function of distance from the uncracked face and lateral distance from the crack plane for the 20 mm crack sample at loads of zero, 8.6 and 17.8 kN.

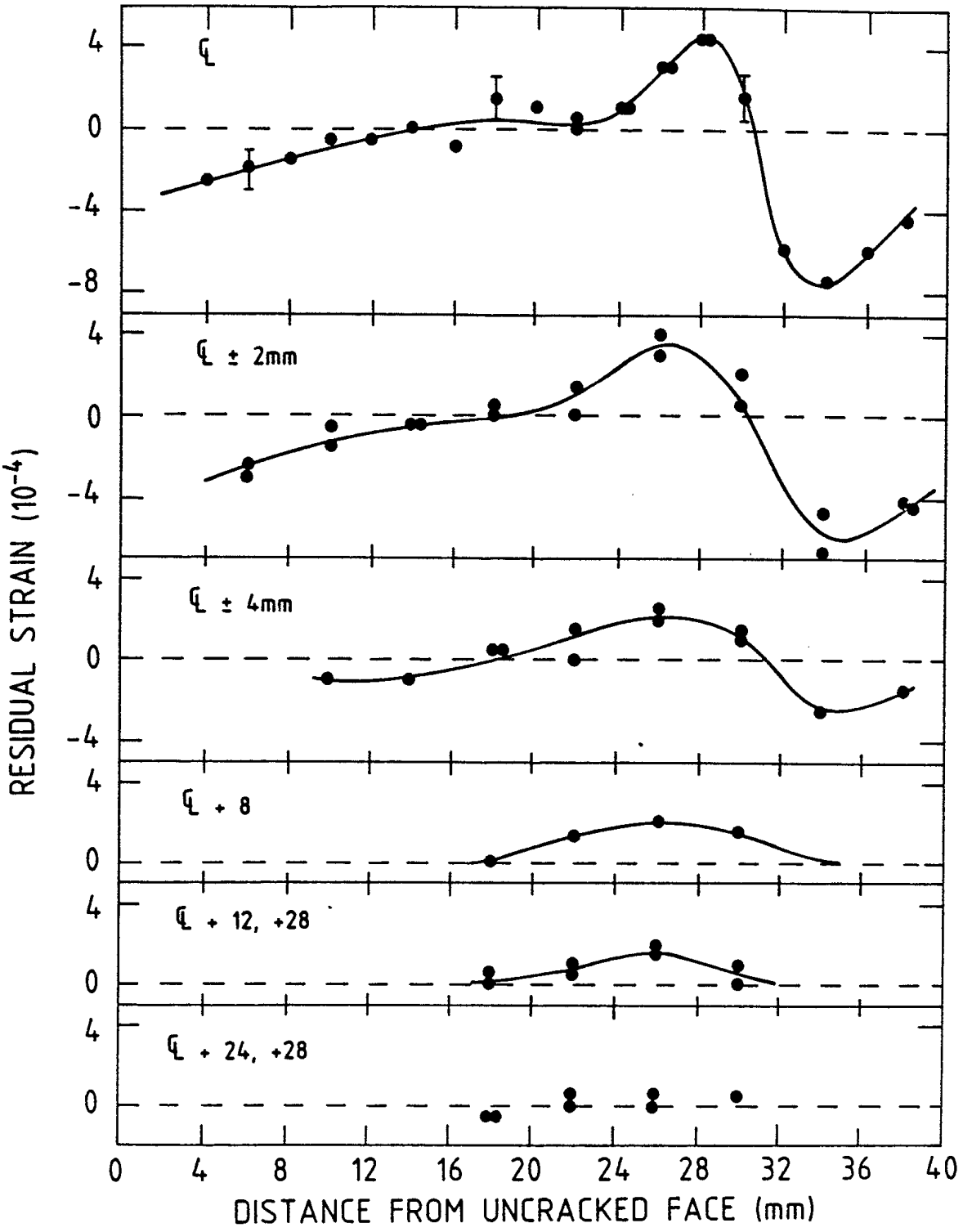

Fig. 5 Residual strains as a function of through-wall position at zero load for the 6 mm shallow crack sample. The different panels denote the results at different lateral displacements from the centreline, C_L, of the crack.

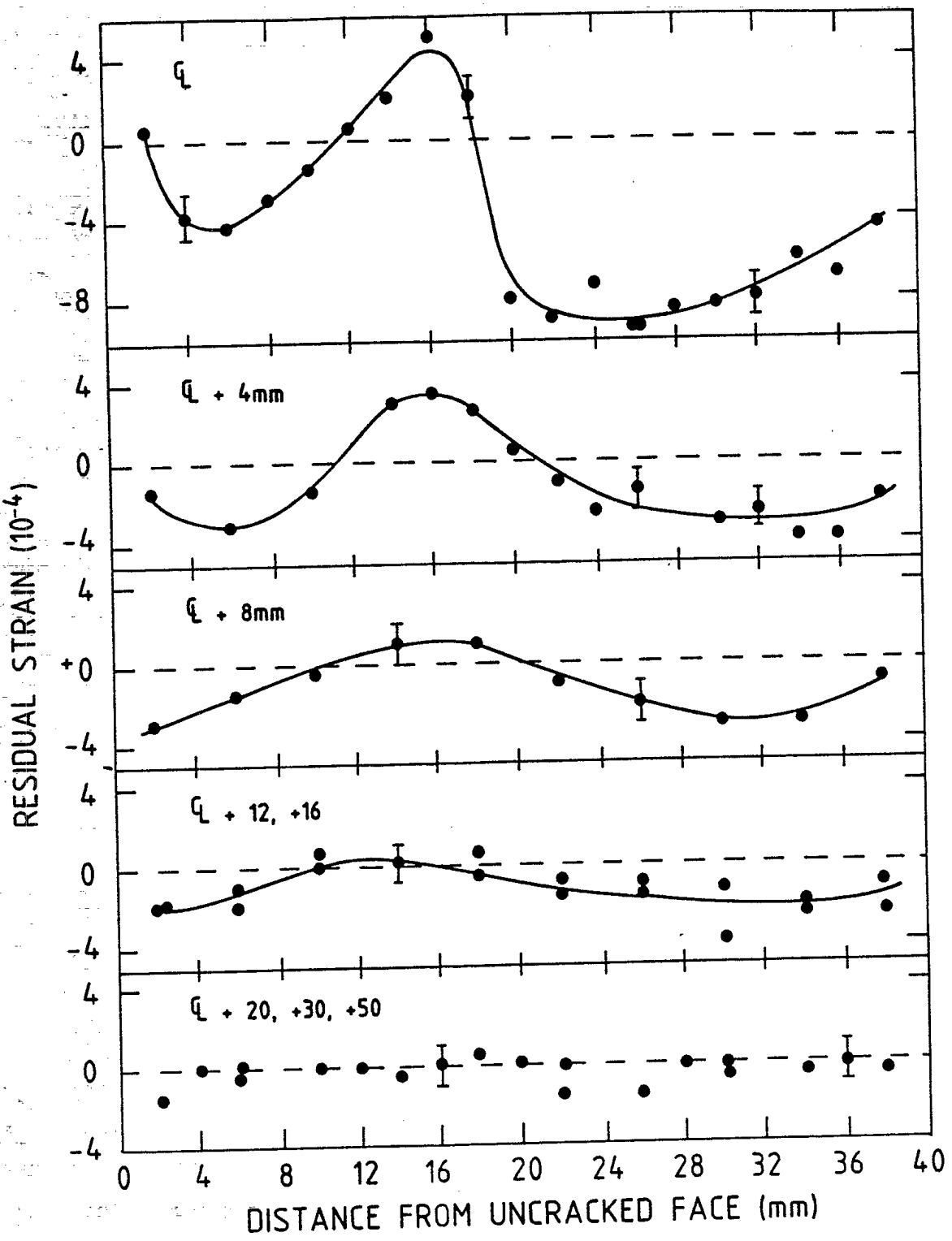

Fig. 6 Residual strains as a function of through-wall position at zero load for the 20 mm deep crack sample. The different panels denote the results at different lateral displacements from the centreline, C_L, of the crack.

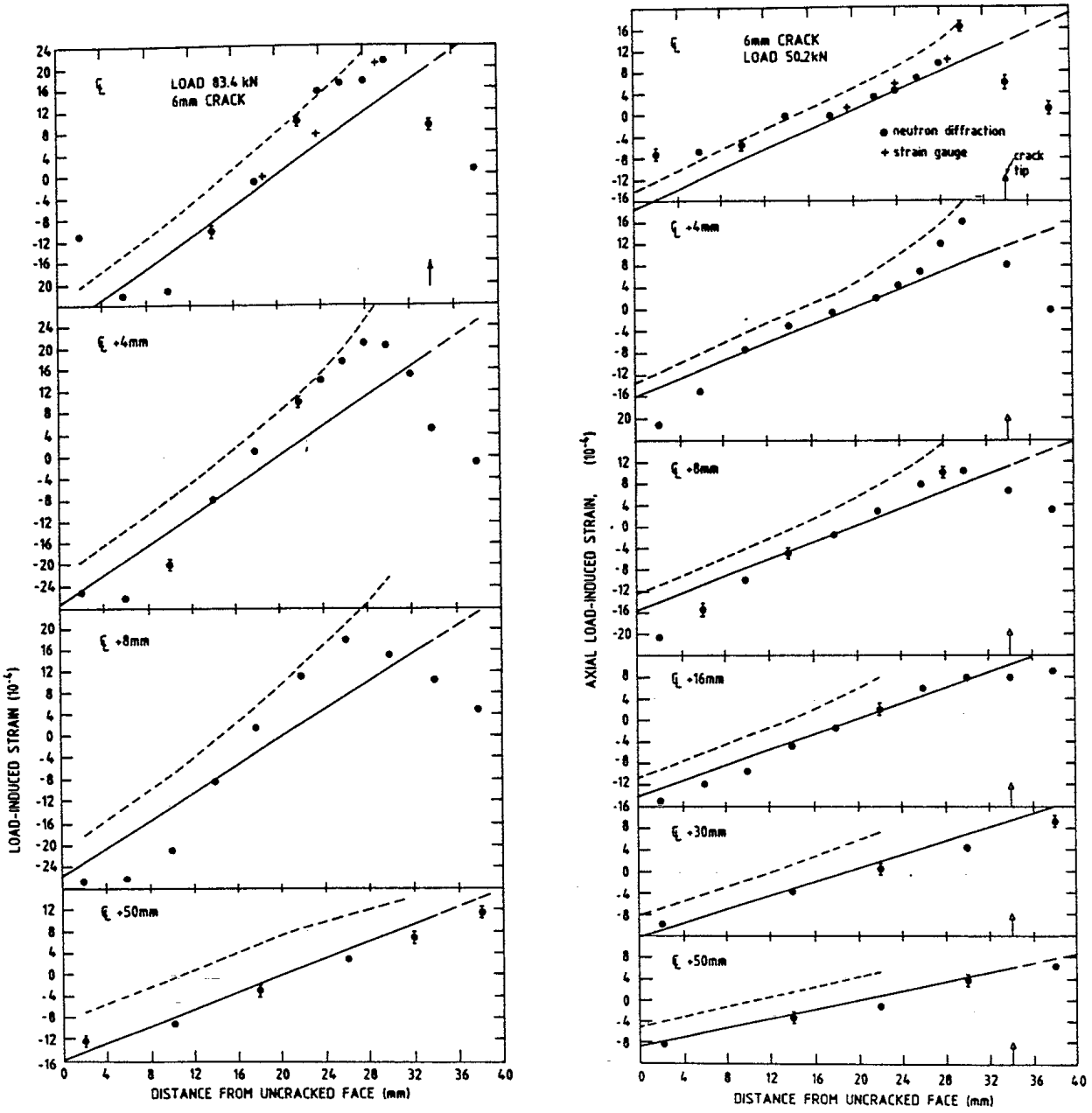

Fig. 7 Load-induced strain measured by neutron diffraction and by strain gauges as a function of position for the 6 mm shallow crack sample. Crosses denote surface strains. The solid curves are calculated from the known applied moment and are indicated by dashed lines at locations closer to the uncracked face than the penetration of the crack. Dash short dashed curves indicate the contribution to the strain from the stress enhancement calculated by linear elastic fracture mechanics.

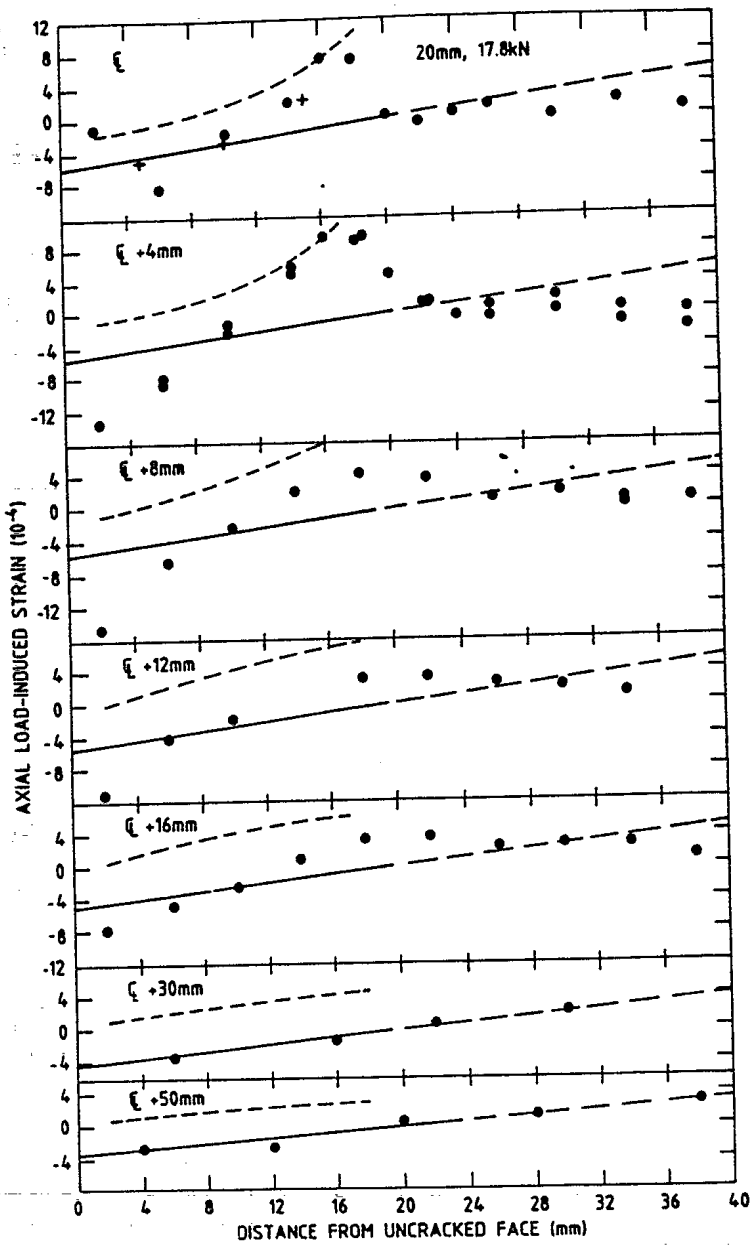

Fig. 8 Load-induced strain measured by neutron diffraction and by strain gauges as a function of position for the 20 mm deep crack sample. Crosses indicate surface strains. The solid curves are calculated from the known applied moment and are indicated by dashed lines at locations closer to the uncracked face than the penetration of the crack. Short dashed curves indicate the contribution to the strain from the stress enhancement calculated by linear elastic fracture mechanics.

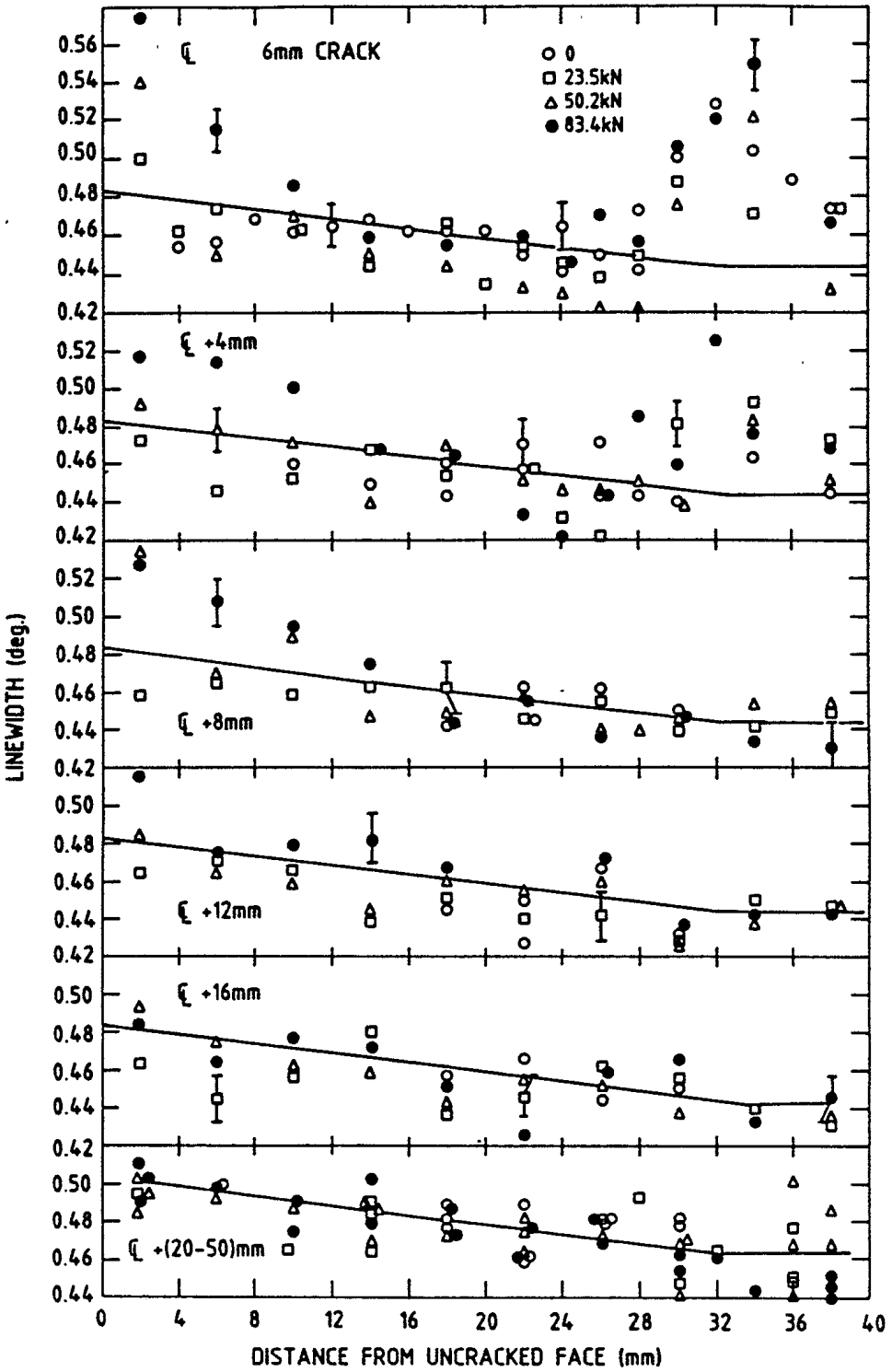

Fig. 9 Measured linewidths as a function of position for the 6 mm shallow crack sample. The solid curve through the data points is the best average width far from the crack which presumably originates in the history of plasticity of the bar. This result is reproduced in the other panels so as to indicate the widths associated with the crack. Enhanced linewidths are observed near the crack tip and opposite the tip on the compressive face.

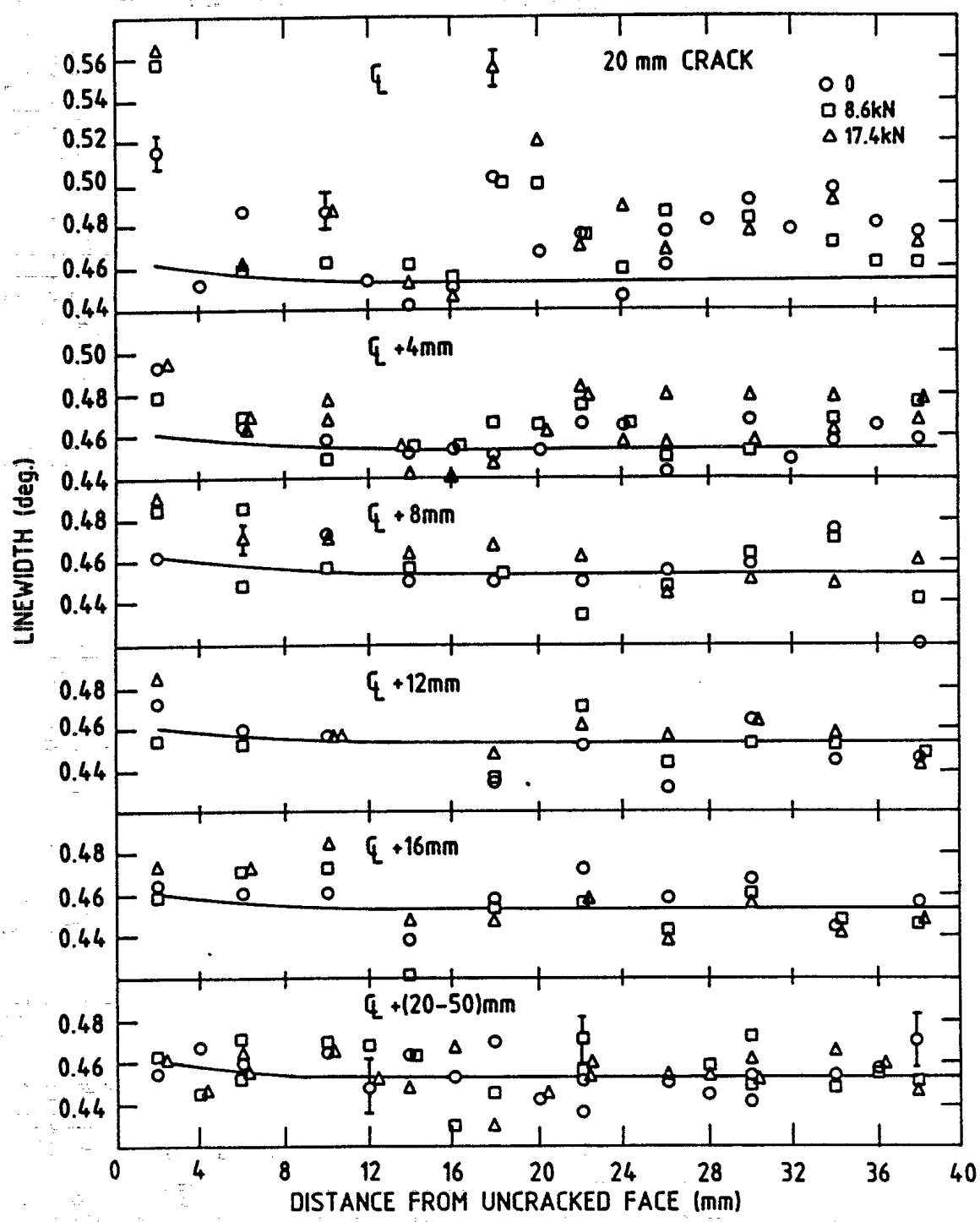

Fig. 10 Measured linewidths as a function of position for the 20 mm crack sample. The solid curve through the data points is the best average width far from the crack, which may originate in the plastic history of the bar. This result is reproduced in the other panels to indicate the widths specifically associated with the crack. Enhanced linewidths are observed near the crack tip and opposite the tip on the compressive face.